Accepted Manuscript

Computer simulations of the activity of RND efflux pumps

Attilio Vittorio Vargiu, Venkata Krishnan Ramaswamy, Giuliano Malloci, Ivana Malvacio, Alessio Atzori, Paolo Ruggerone

PII: S0923-2508(18)30003-2

DOI: 10.1016/j.resmic.2017.12.001

Reference: RESMIC 3630

To appear in: *Research in Microbiology*

Received Date: 30 August 2017

Revised Date: 1 December 2017

Accepted Date: 5 December 2017

Please cite this article as: A.V. Vargiu, V.K. Ramaswamy, G. Malloci, I. Malvacio, A. Atzori, P. Ruggerone, Computer simulations of the activity of RND efflux pumps, *Research in Microbiologoy* (2018), doi: 10.1016/j.resmic.2017.12.001.

This is a PDF file of an unedited manuscript that has been accepted for publication. As a service to our customers we are providing this early version of the manuscript. The manuscript will undergo copyediting, typesetting, and review of the resulting proof before it is published in its final form. Please note that during the production process errors may be discovered which could affect the content, and all legal disclaimers that apply to the journal pertain.

ACCEPTED MANUSCRIPT

For publication

Computer simulations of the activity of RND efflux pumps

Attilio Vittorio Vargiu*, Venkata Krishnan Ramaswamy, Giuliano Malloci, Ivana Malvacio, Alessio Atzori, Paolo Ruggerone*

Department of Physics, University of Cagliari, s.p. 8, Cittadella Universitaria, 09042 Monserrato (CA), Italy

Correspondence: vargiu@dsf.unica.it, paolo.ruggerone@dsf.unica.it

Abstract

The putative mechanism by which bacterial RND-type multidrug efflux pumps recognize and transport their substrates is a complex and fascinating enigma of structural biology. How a single protein can recognize a huge number of unrelated compounds and transport them through one or just a few mechanisms is an amazing feature not yet completely unveiled. The appearance of cooperativity further complicates the understanding of structure-dynamics-activity relationships in these complex machineries. Experimental techniques may have limited access to the molecular determinants and to the energetics of key processes regulating the activity of these pumps. Computer simulations are a complementary approach that can help unveil these features and inspire new experiments. Here we review recent computational studies that addressed the various molecular processes regulating the activity of RND efflux pumps.

ACCEPTED MANUSCRIPT

ACCEPTED MANUSCRIPT

Keywords: Antibiotic resistance; RND efflux pumps; AcrAB-TolC; Molecular dynamics; Molecular docking; Free energy calculations

ACCEPTED MANUSCRIPT

ACCEPTED MANUSCRIPT

1. Introduction

Efflux systems of the resistance-nodulation-cell division (RND) superfamily are a unique family of membrane transport proteins playing a major role in multidrug resistance (MDR) in Gram-negative bacteria [1-5]. They are among the most complex biological machineries ever discovered, connecting the inner and outer membranes through the entire periplasm [1, 6-9], and they crucially contribute to eluding the action of most (in some instances, all) antibiotics [10-13] by shuttling them out of the cell interior [1-4, 14, 5]. Polyspecificity and partial overlap among the substrate specificities of different pumps are striking properties of these proteins [15, 16], making them a key survival tool for bacteria.

The AcrAB-TolC efflux system of *Escherichia coli* is the paradigm model and the most studied RND efflux pump, and the main one in *Enterobacteriaceae* and *Salmonella* Typhimurium [17, 1]. The overall structure of AcrAB-TolC in *E. coli* has been recently resolved [18-20], revealing that the outer membrane trimeric channel TolC is connected to the inner membrane trimer AcrB by a funnel composed of six inner-membrane-anchored AcrA adaptor proteins. A fourth small transmembrane (TM) protein, named AcrZ [21], was recently shown to interact with AcrB in *E. coli* [19], although its biological function is still poorly understood. The second most studied system is represented by the MexAB-OprM complex of the pathogen *Pseudomonas aeruginosa* [22, 1].

The structural features of RND pumps and of their components, as well as their putative function mechanisms, are discussed elsewhere in this special Issue. In this review, we focus our attention only on computational studies performed on RND transporters, referring the interested reader to the available literature on partner

ACCEPTED MANUSCRIPT

proteins (see e.g. [23-28] and on t he simulations of the full tripartite AcrABZ-TolC system [29]).

As concerns the scope of the review, we briefly recall that RND drug/H^+ antiporters are fueled by the proton gradient across the inner membrane, and are involved in the recognition and translocation of a broad range of compounds [30]. Experimental data revealed that the putative active state of AcrB is an asymmetric homotrimer in which monomers assume different conformations, named Loose (L), Tight (T), and Open (O) [or, alternatively, Access (A), Binding (B), Extrusion (C)] [31-33] (Fig. 1). A “functional rotation” mechanism was proposed, explaining substrate export in terms of peristaltic motions induced within the internal channels of the transporter. In the simplest hypothesis (Fig. 2; see, e.g. [34-36] for a more complex picture), recognition of substrates should start at an affinity site, the access pocket (AP), in the L monomer (Fig. 1A-B) [34, 37]. Triggered by substrate binding, a conformational transition from L to T would then occur, accompanied by tight binding of the substrate within a deeper site, the so-called deep or distal pocket (DP) [31-33]. Successively, a second conformational change from T to O (presumed to be the energy-requiring step [38]) should drive displacement of the substrate toward the upper (Funnel) domain through a putative exit gate (hereafter, simply Gate [33]) (Figs. 1, 2). After substrate release, the O conformation would relax back to L (coupled to proton freeing in the cytosol), restarting the cycle. Note that different mechanisms of recognition were proposed for high vs. low molecular mass compounds, involving binding to the AP of monomer L and to the DP of monomer T, respectively [34].

Given the complexity of this process, assessment of the molecular determinants of the mechanism by which RND efflux pumps recognize and export

ACCEPTED MANUSCRIPT

their substrates has proven to be very challenging for experiments. Therefore, it is not surprising that, in the last few years, an increasing number of computational groups began working on these systems. In this review, we address specific features of RND pumps that have been highlighted by computational modeling; therefore, we will not cover all of the computational studies performed on these proteins. Namely, we will recapitulate the major outcomes from selected computational studies (most performed on the AcrB protein of *E. coli*) addressing the mechanisms of remote allosteric coupling, substrate recognition and transport, impact of mutations, and cooperativity [39-57, 36, 58, 59]. Computational studies on inhibitors of the pumps have been recently reviewed by several authors [60-64, 30, 65, 66]; hence, they will not be discussed here.

2.Remote coupling between TM and periplasmic domains of AcrB

The requirement for concerted proton-driven conformational changes in monomers of AcrB was demonstrated by several experiments [67, 68]. On the other hand, there is no agreement on the exact number (1 or 2 per monomer) of protons needed to achieve a full conformational cycle of the pump [36, 6]. In particular, the protonation state of the O monomer is still under debate [36, 69, 70].

The first computational study addressing the relationship between alteration of protonation states in the TM region of AcrB, and conformational rearrangements of the periplasmic region of the protein, was published by Yamane et al. [70]. The authors performed a series of 100 ns long all-atom simulations using all the possible combinations of protonation states of TM aspartates D407 and D408 in monomer O of AcrB. Their simulations demonstrated that alternating the above protonation states induces structural changes in the periplasmic domain of the transporter. Specifically, the authors' findings indicated that the combination D407/D408^{+} was most

ACCEPTED MANUSCRIPT

compatible with the structure of the O state. In contrast, de-protonation of the latter aspartate induced a significant structural transition in the TM region of the protein, suggesting that proton translocation stoichiometry may be one proton per step along the full functional rotation cycle. It must be noted that, due to the relatively short time scale of the simulations (particularly in view of the large size of the system), the observed structural movements involved in an entire functional cycle might be absent/overlooked.

In the same year, Fischer and Kandt [58] performed a series of 100 ns long all-atom MD simulations of AcrB using different protonation states for the L, T and O monomers. Their study highlighted the oscillatory behavior of the AP in L and T conformations and of the Gate in the O structure. They also found that the DP partly collapses in all AcrB monomers in the absence of substrates (although no evidence was obtained supporting the LLL resting state in the absence of substrates), pointing to the possibility of unresolved substrates in some of the asymmetric X-ray structures. Finally, the authors pinpointed the key role of the T676 loop (cyan loop in Fig. 1C), which regulates access to the porter domain, thus playing a crucial role in substrate transport.

Very recently, Jewel et al. used hybrid all-atom/coarse-grained simulations extended to 1 μs to study allosteric effects due to changes in the protonation states within the TM region [69]. Their results confirmed that de-protonation of only D408 (and not D407) induces opening of the entrance cleft between domains PC1 and PC2 (Cleft in Fig. 1C) and closing of the Gate lined by residues Q124 and Y758 (see Table 1). According to these findings, de-protonation of D408 appears to be the main driving force for the transition from the O to L state. Furthermore, the authors' findings also support the symmetric state of AcrB when unbound to substrates.

ACCEPTED MANUSCRIPT

Eicher et al. used X-ray crystallography and computer simulations on wild type and inactive variants of AcrB to investigate its transport mechanism [36]. Intriguingly, a different protonation state than that reported in [70, 69] was indicated as most likely for the O state, whereby D407 and D408 are both protonated. The authors demonstrated that the functional rotation mechanism involves two remote alternating-access conformational cycles within each monomer, one for protons in the TM region and one for substrates in the periplasmic domain. By analyzing the distribution of water molecules in each monomer of AcrB during all-atom MD simulations started from the asymmetric structure of the protein, the authors showed the existence of conformation-dependent water channels within the TM domain. In particular, it was shown that access to the proton relay site lined by D407, D408 and K940 happens from the cytoplasm in the L and O states, as opposed to the T state, where a water wire extends to the periplasm (Fig. 3). A similar conclusion was earlier drawn by Fischer and Kandt [59], who identified three possible routes of proton transfer connecting a continuously hydrated region within the TM to bulk water by one cytoplasmic, and up to three periplasmic, water channels in monomers L and T. Furthermore, they also postulated a proton release event during transition from O to L, and proton uptake in L and/or T or during an intermediate conformation in between T and O.

Clearly, the interaction with the partner protein AcrA ,as well as with several components of a real membrane, not taken into account in any of the aforementioned studies, could significantly alter the conformational distribution of subdomain orientations on the surface of AcrB. In addition, the relatively short timescale of most MD simulations performed thus far can lead to overlooked results. For instance, no significant oscillations were seen in the behavior of the AP and DP in a recent series

ACCEPTED MANUSCRIPT

of μs long unbiased all-atom MD simulations of AcrB and AcrD (the second major transporter in *Enterobacteriaceae* and *Salmonella* [17, 1]) [39]. In the absence of substrates, both pockets partly collapsed with respect to the conformation seen in the X-ray crystal (AcrB) and in the homology modeling-derived (AcrD) structures. Further studies including the effects from ancillary factors (partner proteins and membrane composition) are therefore needed to better understand remote coupling and general conformational dynamics related to the functioning of RND transporters.

3.Molecular determinants of polyspecificity

The first computational study reporting on the binding of several compounds to AcrB (including substrates, inhibitors and non-substrates) [71] employed the docking software Autodock VINA [72]. The authors found that many compounds bind within a narrow groove at one end of the DP of monomer T (groove binders), while some prefer to bind to a wide cave at the other end of the pocket (cave binders), and a third group of compounds were found docked in between the groove and the cave (mixed binders). The distinction between groove and cave binders was supported by labeling and competition experiments, although it became somewhat blurred in a subsequent study combining docking, all-atom MD simulations and free energy calculations [46]. The latter study also confirmed the presence of a very wide pocket of exceptional promiscuity exploiting virtually all interaction types to stabilize binding of different and unrelated compounds. In particular, residues F136, Q176, F178, I277, V612, F615, R620 and F628 were shown to contribute most to the stabilization of substrates (Fig. 4), in good agreement with transport studies performed in intact-cell experiments [73].

The presence of two “multifunctional-sites” (MFSs – able to bind aromatic, hydrophobic, and polar groups) on the two ends of the DP was earlier demonstrated

ACCEPTED MANUSCRIPT

by Imai et al. [74], who also showed that binding sites are different in each AcrB monomer, implying that a drug avoids being trapped in one location through site-specific interactions during pump cycling. Imai and coauthors also showed that AcrB substrates are stabilized by a complicated free-energy balance originating from weakly polar and weakly hydrophobic surroundings, a finding compatible with [46] and with the multisite drug oscillation hypothesis proposed to explain polyspecificity of RND transporters [6]. Interestingly, this hypothesis is consistent with a recent computational study employing Markov chain Monte Carlo methods to show how diffuse binding of solvents, acriflavine, and minocycline to AcrB contributes significantly to their total affinity [75].

In 2012, Ruggerone and co-workers [47] performed the first computational study providing a molecular rationale for the experimental evidence indicating two relatively similar antibiotics, meropenem and imipenem, respectively, as good and poor substrates of MexB of *P. aeruginosa*. By means of docking calculations, two affinity sites were identified and characterized in the periplasmic domain, sharing strong similarities (in terms of sequence and structure) with the AP and DP of AcrB. Free energy estimates performed over the all-atom MD simulation trajectories of the top-ranked docking poses indicated that meropenem has a higher affinity to the DP than imipenem, while both compounds are weakly bound to the AP. Moreover, it was shown that the hydration properties of the non-pharmacophore moiety of the two compounds (imipenem being more hydrated than meropenem) are mainly responsible for their different interaction with MexB.

Very recently, the same group investigated the molecular determinants behind the different substrate specificities of RND transporters AcrB and AcrD of *Escherichia coli* [39]. A wide comparative analysis of physico-chemical and topographical

ACCEPTED MANUSCRIPT

properties of the two main binding pockets (AP and DP within L and T conformations, respectively) revealed major differences between the two proteins, rationalizing their different substrate specificities. In particular, a higher number of MFSs was identified within the DP and at the interface between the two pockets in AcrB than in AcrD, in line with the higher polyspecificity of the first protein (Fig. 5). The distal pocket of AcrD is mainly lined by hydrogen-bond donors/acceptors, while the percentage of hydrophobic fragments is relatively low. The MFSs identified within the DP of AcrB are in good agreement with the data reported in [74], while some of the MFSs identified in AcrD are close to the residues recognized as crucial for the recognition of anionic beta-lactams [76].

4.Mechanisms of substrate transport

While the previous studies employed docking and mostly standard MD techniques, addressing coupling between conformational changes of RND proteins and transport of compounds often required the use of more advanced computational methodologies. Several studies have been performed to unveil the molecular details of uptake and transport of substrates by RND transporters. The first computational studies supporting the functional rotation hypothesis were published in 2010 [50, 57]. In [57], an ad hoc coarse-grained model of the AcrB pore domain and of minocycline was employed to directly observe extrusion of the substrate during the T to O transition. The study also indicated that protonation of the drug-bound monomer drives functional rotation.

In [50], biased MD simulations were performed on a full all-atom model of AcrB in complex with doxorubicin bound within the DP of monomer T, so as to mimic the displacement of the substrate along the T to O step of the functional rotation. Although full extrusion was expectedly not captured within the relatively short

ACCEPTED MANUSCRIPT

timescale of these simulations (a few tens of ns at most), a translocation of about 10 Å was observed towards the Gate. A zipper-like squeezing of this site induced displacement of doxorubicin from the DP, concomitant with the opening of the channel between this pocket and the Gate, which was also necessary in order to displace the ligand.

In a subsequent study [49] the same authors performed further biased MD simulations to demonstrate the presence of a flux of water molecules from the DP toward the Gate during the T to O step of functional rotation, thus highlighting a lubricant action of water, which smooths the interactions between the substrate and AcrB. Such a flux facilitates substrate diffusion along the extrusion pathway, and could symbolize a very general mechanism for polyspecific transport.

Feng and coauthors also investigated the interaction of AcrB with its substrates, namely erythromycin, rifampicin and minocycline [55]. They described unidirectional peristaltic movements of rifampicin and erythromycin from the AP to the DP in monomer L, and of minocycline from the DP towards the Gate in monomer T. Due to the use of relatively short unbiased simulations, the movements of the compounds were, however, shorter than those seen in [49, 50].

An effort at simulating the translocation of compounds from the DP to the funnel region of AcrB was recently made by Zuo and Weng [51], who performed targeted MD simulations [77] of the T to O conformational change in the protein, followed by steered MD simulations [78, 79] to induce displacement of doxorubicin and of the AcrB inhibitor D13-9001 [80]. The authors found that, with respect to doxorubicin, the interaction of D13-9001 with the phenylalanine-rich cage within the DP (aka hydrophobic trap [81]) resulted in delayed dissociation from the pocket. The same group also performed adaptive bias force [82] MD simulations to investigate

ACCEPTED MANUSCRIPT

translocation of doxorubicin from the vestibule to the DP of monomer T (Fig. 1) [52]. The authors calculated the free energy profile associated with translocation of the substrate across this pathway, which reveals that doxorubicin has comparable affinities for AP and DP and overcomes a 3 kcal/mol free energy barrier to transit between them. In addition, fairly stable binding was possible also at the vestibule of monomer T. The results of Zuo and coworkers detailed a stepwise substrate binding and translocation process that fits well into the framework of the functional rotation mechanism, and indicated that low molecular mass compounds such as doxorubicin could bind the DP of monomer T without prior binding to the AP, as suggested earlier [34].

Concerning the uptake of substrates by RND transporters, this process was first investigated in 2013 by Yao and collaborators, who used coarse-grained MD simulations (coupled with mutagenesis experiments) to map the drug entry pathways in AcrB [56]. Interestingly, three main uptake pathways were identified, one starting from the external cleft between subdomains PC1 and PC2 and two starting from the vestibule (Fig. 6). Importantly, one of the vestibule pathways was not deducible from the X-ray structure, and only became accessible by direct simulations of drug uptake. Moreover, site-directed mutagenesis confirmed that mutations of residues located along this new pathway affected the efflux efficiency of AcrB in *E. coli*, supporting its relevance in vivo. The pathway preferences of model drugs were found to be significantly different depending on their properties, namely on their mass, hydrophobicity and lipophilicity. In particular, drugs that are small and/or both strongly hydrophobic and lipophilic were preferentially taken in via the vestibule paths, while bulkier drugs and/or drugs with a large hydrophilic surface favored the Cleft path (Fig. 6B).

ACCEPTED MANUSCRIPT

5.Effect of mutations on recognition and transport

RND transporters, in particular AcrB of *E. coli*, have been the subject of many mutagenesis studies by several labs worldwide (see e.g. [83-88] to cite a few), which aimed to validate hypotheses on binding and transport by these proteins. A number of computational works were performed in order to rationalize the huge amount of findings revealed by these studies. In 2011, docking calculations combined with standard and biased all-atom MD simulations were performed to study the effect of the F610A substitution in AcrB [48]. This substitution was known to increase in vitro the susceptibility of *E. coli* to almost all antibiotics [84] due to delayed efflux [83]. According to results in [48], the removal of the bulky phenylalanine at the bottom of the DP allowed sliding of doxorubicin by ~5 Å within the hydrophobic trap lined by F136, F178, F615 and F628 (Table 1). This resulted in better packing of the antibiotic within the trap, thereby increasing its affinity to the DP (Fig. 7), which led to the proposal that the inhibitory effect associated with the F610A mutation was due to the increased dwelling time of the substrate within the AcrB variant. Consistent with this hypothesis, no significant movement of doxorubicin towards the Gate was observed upon induction of the T to O conformational change in the AcrB variant. The authors concluded that the F610A mutation might impair AcrB functioning by either hindering conformational changes in the protein or interfering with the extrusion of substrates due to their improved binding to the hydrophobic trap. These findings were later confirmed for minocycline [30], the only other antibiotic experimentally found to bind to the DP of monomer T at that time.

Another key region related to transport of substrates in AcrB is the so-called Phe617- or G- or switch-loop [46, 34, 37] (Fig. 1C), which acts as a gate between the AP and the DP and was shown to impair functioning of AcrB if rigidified by site-

ACCEPTED MANUSCRIPT

directed mutagenesis [34, 37]. Feng et al. performed MD simulations confirming that the mutations of G616P and G619P could indeed prevent movement of the F617-loop compared to the wild type protein [55]. Müller et al. [89] proved that the single or combined mutations of G614P and G616P affected transport of several substrates, while G619P or G621P mutants were able to preserve an intermediate efflux activity. These results suggest that only a defined structural asymmetry within the G-loop seems to have a relevant effect on the transport of substrates between the AP and DP. The restricted switch loop movement observed in [55] can therefore be mainly attributed to the G616P mutation.

A third mutation, G288D, was reported to decrease the susceptibility of *Salmonella* strains to ciprofloxacin by increased efflux, while increasing susceptibility to other drugs (including doxorubicin) by decreased efflux [43]. Computer simulations helped rationalize these findings by showing how the mutation heavily affects the structure, dynamics and hydration properties of the DP of AcrB, crucially altering its specificity for antibacterial drugs [43]. In particular, it was found that ciprofloxacin binds to a region of the DP that is relatively far away from the mutation site [46, 43], while doxorubicin binds exactly to the same region observed in X-ray structures [31, 37].

6.Molecular determinants of cooperativity

Nikaido and co-workers performed the first evaluation of efflux kinetics in AcrB, demonstrating strong positive cooperativity for transport of many cephalosporins [90]. That study was followed by a similar one on penicillins [91], by another investigating the effect of additional ligands on the AcrB substrates [45], and by another investigating the kinetics of the inhibitor PAβN and its aminoacyl β-naphthylamides homologues [41]. In the latter two studies, computer simulations

ACCEPTED MANUSCRIPT

were also performed to support the experimental findings.

In [45], docking and MD simulations were performed to show how the simultaneous presence of substrates such as chloramphenicol, benzene, cyclohexane, or Arg β-naphthylamide enhanced the efflux of cephalosporins in AcrB, and even more in its V139F variant. Benzene and nitrocefin were found to bind simultaneously to the DP in both wild type and mutant AcrB, and nitrocefin was shown to be significantly displaced toward the Gate by the binding of benzene. On the basis of these findings, it was proposed that the efflux of cephalosporins, which presumably bind to a different subsite within the large DP, can become facilitated by the rapid pumping out of solvent or chloramphenicol molecules and/or the binding of solvents even to the cephalosporin-free monomer, which could accelerate AcrB conformational changes necessary for substrate extrusion.

In [41], it was suggested that the positive cooperativity and sigmoidal kinetics characterizing the efflux of some compounds by AcrB are due to their loose binding to the transporter. If a substrate of AcrB, like aminoacyl β-naphthylamides and some β-lactams, binds loosely to the DP, then the entry of a second compound into the AP of L or T monomers could lead to a situation of simultaneous binding that could promote positive cooperativity. In contrast, substrates such as nitrocefin, which binds tightly to the DP (but out of the hydrophobic trap), may not need additional binding to activate the transporter. In addition, in [41] the modulation of efflux of nitrocefin (a groove binder [71, 46]) by aminoacyl β-naphthylamides was rationalized in terms of their mode of binding to AcrB. Specifically, L-alanyl-β-naphthylamide (Ala-Naph), which acts as a stimulator of efflux, likely exploits a mechanism similar to that proposed for solvents such as benzene [45]. Arg-Naph, also behaving as a stimulator, binds out of the groove and only peripherally to the hydrophobic trap;

ACCEPTED MANUSCRIPT

thus, it is unlikely to interfere with the binding of nitrocefin. Furthermore, the effect of the double-positive charge of Arg-Naph on the binding of negatively charged nitrocefin may also contribute to stimulation of its efflux. Phe-Naph, which acts as an inhibitor of nitrocefin efflux, instead significantly binds to the hydrophobic trap, and its phenylalanine extends into the groove, likely hindering binding of nitrocefin.

7.Concluding remarks and future directions

Since the publication of the first computational study on RND transporters less than a decade ago [50], an increasing number of research labs have been getting involved in studies on these huge, complex and fascinating machineries. Thanks also to these studies, many details regulating export of substrates by RND transporters were unveiled and/or rationalized. Clearly, several aspects including those discussed here (in addition to better understanding of inhibition routes) need further clarification. Among these, the presence of possible alternative uptake routes of substrates, as well as a deeper understanding of the link between route preferences and physico-chemical features of different compounds, need further elucidation. While this problem has been addressed by means of a simplified description of the main players involved [56], drug design efforts would greatly benefit from a more detailed (that is, atomistic) description of the process. Concerning the molecular determinants behind the functional rotation mechanism, no study has yet fully addressed how the conformational changes induced in AcrB facilitate diffusion of substrates towards the funnel domain. Thus, the feasibility of the proposed functional rotation mechanism remains to be established; henceforth, the development of computational protocols to address this challenge is highly necessary. Finally, none of the studies reported here were carried out on whole efflux pumps. Although challenging, a better understanding of the impact upon and role of partner proteins in

ACCEPTED MANUSCRIPT

376 the whole efflux process is definitively worth considering.

ACCEPTED MANUSCRIPT

ACCEPTED MANUSCRIPT

377 ***References***

378 [1] Li X-Z, Plésiat P, Nikaido H. The Challenge of Efflux-Mediated Antibiotic
379 Resistance in Gram-Negative Bacteria. Clin. Microbiol. Rev. 2015;28:337-418.
380 [2] Blair JMA, Richmond GE, Piddock LJV. Multidrug efflux pumps in Gram-negative
381 bacteria and their role in antibiotic resistance. Future Microbiol. 2014;9:1165-77.
382 [3] Sun J, Deng Z, Yan A. Bacterial multidrug efflux pumps: mechanisms, physiology
383 and pharmacological exploitations. Biochem. Biophys. Res. Commun. 2014;453:254-
384 67.
385 [4] Hernando-Amado S, Blanco P, Alcalde-Rico M, Corona F, Reales-Calderon JA,
386 Sanchez MB, et al. Multidrug efflux pumps as main players in intrinsic and acquired
387 resistance to antimicrobials. Drug Resist. Updates 2016;28:13-27.
388 [5] Chitsaz M, Brown MH. The role played by drug efflux pumps in bacterial multidrug
389 resistance. Essays Biochem. 2017;61:127-39.
390 [6] Yamaguchi A, Nakashima R, Sakurai K. Structural basis of RND-type multidrug
391 exporters. Front. Microbiol. 2015;6:327.
392 [7] Zgurskaya HI, Weeks JW, Ntreh AT, Nickels LM, Wolloscheck D. Mechanism of
393 coupling drug transport reactions located in two different membranes. Front.
394 Microbiol. 2015;6:100.
395 [8] Poole K. Efflux pumps as antimicrobial resistance mechanisms. Ann. Med.
396 2007;39:162-76.
397 [9] Du D, van Veen HW, Murakami S, Pos KM, Luisi BF. Structure, mechanism and
398 cooperation of bacterial multidrug transporters. Curr. Opin. Struct. Biol. 2015;33:76-
399 91.
400 [10] Hede K. Antibiotic resistance: An infectious arms race. Nature 2014;509:S2-S3.

ACCEPTED MANUSCRIPT

401 [11] Brown ED, Wright GD. Antibacterial drug discovery in the resistance era. Nature
402 2016;529:336-43.
403 [12] Courvalin P. Why is antibiotic resistance a deadly emerging disease? Clin.
404 Microbiol. Infect. 2016;22:405-7.
405 [13] Inoue H, Minghui R. Bulletin of the World Health Organization. 2017, p. 242.
406 [14] Venter H, Mowla R, Ohene-Agyei T, Ma S. RND-type Drug Efflux Pumps from
407 Gram-negative bacteria: Molecular Mechanism and Inhibition. Front. Microbiol.
408 2015;6.
409 [15] Tal N, Schuldiner S. A coordinated network of transporters with overlapping
410 specificities provides a robust survival strategy. Proc. Natl. Acad. Sci. U. S. A.
411 2009;106:9051-6.
412 [16] Zhou G, Shi Q-S, Huang X-M, Xie X-B. The three bacterial lines of defense
413 against antimicrobial agents. Int. J. Mol. Sci. 2015;16:21711-33.
414 [17] Andersen J, He G-X, Kakarla P, KC R, Kumar S, Lakra W, et al. Multidrug Efflux
415 Pumps from Enterobacteriaceae, Vibrio cholerae and Staphylococcus aureus
416 Bacterial Food Pathogens. Int. J. Environ. Res. Public. Health 2015;12:1487.
417 [18] Wang Z, Fan G, Hryc CF, Blaza JN, Serysheva II, Schmid MF, et al. An allosteric
418 transport mechanism for the AcrAB-TolC multidrug efflux pump. eLife
419 2017;6:e24905.
420 [19] Du D, Wang Z, James NR, Voss JE, Klimont E, Ohene-Agyei T, et al. Structure
421 of the AcrAB-TolC multidrug efflux pump. Nature 2014;509:512-5.
422 [20] Jin-Sik K, Hyeongseop J, Saemee S, Hye-Yeon K, Kangseok L, Jaekyung H, et
423 al. Structure of the Tripartite Multidrug Efflux Pump AcrAB-TolC Suggests an
424 Alternative Assembly Mode. Mol. Cells 2015;38:180-6.

ACCEPTED MANUSCRIPT

425 [21] Hobbs EC, Yin X, Paul BJ, Astarita JL, Storz G. Conserved small protein
426 associates with the multidrug efflux pump AcrB and differentially affects antibiotic
427 resistance. Proc. Natl. Acad. Sci. U. S. A. 2012;109:16696-701.
428 [22] Poole K. Pseudomonas aeruginosa: resistance to the max. Front. Microbiol.
429 2011;2:90-102.
430 [23] Vaccaro L, Koronakis V, Sansom MSP. Flexibility in a drug transport accessory
431 protein: Molecular dynamics simulations of MexA. Biophys. J. 2006;91:558-64.
432 [24] Vaccaro L, Scott KA, Sansom MSP. Gating at Both Ends and Breathing in the
433 Middle: Conformational Dynamics of TolC. Biophys. J. 2008;95:5681-91.
434 [25] Raunest M, Kandt C. Locked on One Side Only: Ground State Dynamics of the
435 Outer Membrane Efflux Duct TolC. Biochemistry 2012;51:1719-29.
436 [26] Koch DC, Raunest M, Harder T, Kandt C. Unilateral Access Regulation: Ground
437 State Dynamics of the Pseudomonas aeruginosa Outer Membrane Efflux Duct OprM.
438 Biochemistry 2013;52:178-87.
439 [27] Schulz R, Kleinekathöfer U. Transitions between closed and open conformations
440 of TolC: the effects of ions in simulations. Biophys. J. 2009;96:3116-25.
441 [28] Wang B, Weng J, Wang W. Free energy profiles of ion permeation and
442 doxorubicin translocation in TolC. J. Theor. Comput. Chem. 2014;13:1450031.
443 [29] Hsu PC, Samsudin MF, Shearer J, Khalid S. It's Complicated: Curvature,
444 Diffusion and Lipid Sorting Within the Two Membranes of Escherichia Coli. J. Phys.
445 Chem. Lett. 2017;8:5513-8.
446 [30] Ruggerone P, Murakami S, Pos KM, Vargiu AV. RND Efflux Pumps: Structural
447 Information Translated into Function and Inhibition Mechanisms. Curr. Top. Med.
448 Chem. 2013;13:3079-100.

ACCEPTED MANUSCRIPT

449 [31] Murakami S, Nakashima R, Yamashita E, Matsumoto T, Yamaguchi A. Crystal
450 structures of a multidrug transporter reveal a functionally rotating mechanism. Nature
451 2006;443:173-9.
452 [32] Seeger MA, Schiefner A, Eicher T, Verrey F, Diederichs K, Pos KM. Structural
453 Asymmetry of AcrB Trimer Suggests a Peristaltic Pump Mechanism. Science
454 2006;313:1295-8.
455 [33] Sennhauser G, Amstutz P, Briand C, Storchenegger O, Grütter MG. Drug export
456 pathway of multidrug exporter AcrB revealed by DARPin inhibitors. PLoS Biol.
457 2007;5:e7.
458 [34] Nakashima R, Sakurai K, Yamasaki S, Nishino K, Yamaguchi A. Structures of
459 the multidrug exporter AcrB reveal a proximal multisite drug-binding pocket. Nature
460 2011;480:565-9.
461 [35] Oswald C, Tam H-K, Pos KM. Transport of lipophilic carboxylates is mediated by
462 transmembrane helix 2 in multidrug transporter AcrB. Nat. Commun. 2016;7:13819.
463 [36] Eicher T, Seeger MA, Anselmi C, Zhou W, Brandstätter L, Verrey F, et al.
464 Coupling of remote alternating-access transport mechanisms for protons and
465 substrates in the multidrug efflux pump AcrB. eLife 2014;3:e03145.
466 [37] Eicher T, Cha H-j, Seeger MA, Brandstaetter L, El-Delik J, Bohnert JA, et al.
467 Transport of drugs by the multidrug transporter AcrB involves an access and a deep
468 binding pocket that are separated by a switch-loop. Proc. Natl. Acad. Sci. U. S. A.
469 2012;109:5687-92.
470 [38] Seeger MA, Diederichs K, Eicher T, Brandstatter L, Schiefner A, Verrey F, et al.
471 The AcrB Efflux Pump: Conformational Cycling and Peristalsis Lead to Multidrug
472 Resistance. Curr. Drug Targets 2008;9:729-49.

ACCEPTED MANUSCRIPT

473 [39] Ramaswamy VK, Vargiu AV, Malloci G, Dreier J, Ruggerone P. Molecular
474 Rationale behind the Differential Substrate Specificity of Bacterial RND Multidrug
475 Transporters. Sci. Rep. 2017;7.
476 [40] Sjuts H, Vargiu AV, Kwasny SM, Nguyen ST, Kim H-S, Ding X, et al. Molecular
477 basis for inhibition of AcrB multidrug efflux pump by novel and powerful
478 pyranopyridine derivatives. Proc. Natl. Acad. Sci. U. S. A. 2016;113:3509-14.
479 [41] Kinana AD, Vargiu AV, May T, Nikaido H. Aminoacyl β-naphthylamides as
480 substrates and modulators of AcrB multidrug efflux pump. Proc. Natl. Acad. Sci. U. S.
481 A. 2016;113:1405-10.
482 [42] Schulz R, Vargiu AV, Ruggerone P, Kleinekathoefer U. Computational Study of
483 Correlated Domain Motions in the AcrB Efflux Transporter. BioMed Res. Int.
484 2015;2015:12.
485 [43] Blair JMA, Bavro VN, Ricci V, Modi N, Cacciotto P, Kleinekathoefer U, et al.
486 AcrB drug-binding pocket substitution confers clinically relevant resistance and
487 altered substrate specificity. Proc. Natl. Acad. Sci. U. S. A. 2015;112:3511-6.
488 [44] Vargiu AV, Ruggerone P, Opperman TJ, Nguyen ST, Nikaido H. Molecular
489 Mechanism of MBX2319 Inhibition of Escherichia coli AcrB Multidrug Efflux Pump
490 and Comparison with Other Inhibitors. Antimicrob. Agents Chemother. 2014;58:6224-
491 34.
492 [45] Kinana AD, Vargiu AV, Nikaido H. Some Ligands Enhance the Efflux of Other
493 Ligands by the Escherichia coli Multidrug Pump AcrB. Biochemistry 2013;52:8342-
494 51.
495 [46] Vargiu AV, Nikaido H. Multidrug binding properties of the AcrB efflux pump
496 characterized by molecular dynamics simulations. Proc. Natl. Acad. Sci. U. S. A.
497 2012;109:20637-42.

ACCEPTED MANUSCRIPT

498 [47] Collu F, Vargiu AV, Dreier J, Cascella M, Ruggerone P. Recognition of
499 Imipenem and Meropenem by the RND-Transporter MexB Studied by Computer
500 Simulations. J. Am. Chem. Soc. 2012;134:19146-58.
501 [48] Vargiu AV, Collu F, Schulz R, Pos KM, Zacharias M, Kleinekathöfer U, et al.
502 Effect of the F610A Mutation on Substrate Extrusion in the AcrB Transporter:
503 Explanation and Rationale by Molecular Dynamics Simulations. J. Am. Chem. Soc.
504 2011;133:10704-7.
505 [49] Schulz R, Vargiu AV, Ruggerone P, Kleinekathöfer U. Role of Water during the
506 Extrusion of Substrates by the Efflux Transporter AcrB. J. Phys. Chem. B
507 2011;115:8278-87.
508 [50] Schulz R, Vargiu AV, Collu F, Kleinekathöfer U, Ruggerone P. Functional
509 Rotation of the Transporter AcrB: Insights into Drug Extrusion from Simulations.
510 PLoS Comput. Biol. 2010;6:e1000806.
511 [51] Zuo Z, Weng J, Wang W. Insights into the Inhibitory Mechanism of D13-9001 to
512 the Multidrug Transporter AcrB through Molecular Dynamics Simulations. J. Phys.
513 Chem. B 2016;120:2145-54.
514 [52] Zuo Z, Wang B, Weng J, Wang W. Stepwise substrate translocation mechanism
515 revealed by free energy calculations of doxorubicin in the multidrug transporter AcrB.
516 Sci. Rep. 2015;5:13905.
517 [53] Wang B, Weng J, Wang W. Substrate binding accelerates the conformational
518 transitions and substrate dissociation in multidrug efflux transporter AcrB. Front.
519 Microbiol. 2015;6:302.
520 [54] Wang B, Weng J, Fan K, Wang W. Interdomain Flexibility and pH-Induced
521 Conformational Changes of AcrA Revealed by Molecular Dynamics Simulations. J.
522 Phys. Chem. B 2012;116:3411-20.

ACCEPTED MANUSCRIPT

523 [55] Feng Z, Hou T, Li Y. Unidirectional peristaltic movement in multisite drug binding
524 pocket of AcrB from molecular dynamics simulations. Mol. BioSyst. 2012;8:2699-709.
525 [56] Yao X-Q, Kimura N, Murakami S, Takada S. Drug Uptake Pathways of Multidrug
526 Transporter AcrB Studied by Molecular Simulations and Site-Directed Mutagenesis
527 Experiments. J. Am. Chem. Soc. 2013;135:7474-85.
528 [57] Yao X-Q, Kenzaki H, Murakami S, Takada S. Drug export and allosteric coupling
529 in a multidrug transporter revealed by molecular simulations. Nat. Commun.
530 2010;1:117.
531 [58] Fischer N, Kandt C. Porter domain opening and closing motions in the multidrug
532 efflux transporter AcrB. BBA - Biomembr. 2013;1828:632-41.
533 [59] Fischer N, Kandt C. Three ways in, one way out: Water dynamics in the trans-
534 membrane domains of the inner membrane translocase AcrB. Proteins: Struct.,
535 Funct., Bioinf. 2011;79:2871-85.
536 [60] Aron Z, Opperman TJ. Optimization of a novel series of pyranopyridine RND
537 efflux pump inhibitors. Curr. Opin. Microbiol. 2016;33:1-6.
538 [61] Opperman T, Nguyen S. Recent advances toward a molecular mechanism of
539 efflux pump inhibition. Front. Microbiol. 2015;6.
540 [62] Ramaswamy VK, Cacciotto P, Malloci G, Vargiu AV, Ruggerone P.
541 Computational modelling of efflux pumps and their inhibitors. Essays Biochem.
542 2017;61:141-56.
543 [63] Ramaswamy VK, Cacciotto P, Malloci G, Ruggerone P, Vargiu AV. Multidrug
544 Efflux Pumps and Their Inhibitors Characterized by Computational Modeling. in: X-Z
545 Li, CA Elkins and HI Zgurskaya (Eds.), Efflux-Mediated Antimicrobial Resistance in
546 Bacteria: Mechanisms, Regulation and Clinical Implications, Adis, Cham, 2016, pp.
547 797-831.

ACCEPTED MANUSCRIPT

548 [64] Ruggerone P, Vargiu AV, Collu F, Fischer N, Kandt C. Molecular Dynamics
549 Computer Simulations of Multidrug RND Efflux Pumps. Comput. Struct. Biotechnol. J.
550 2013;5:e201302008-e.
551 [65] Jamshidi S, Sutton JM, Rahman KM. An overview of bacterial efflux pumps and
552 computational approaches to study efflux pump inhibitors. Future Med. Chem.
553 2016;8:195-210.
554 [66] Aron Z, Opperman TJ. The hydrophobic trap, the Achilles heel of RND efflux
555 pumps. Res. Microbiol. 2017.
556 [67] Seeger MA, Von Ballmoos C, Eicher T, Brandstätter L, Verrey F, Diederichs K,
557 et al. Engineered disulfide bonds support the functional rotation mechanism of
558 multidrug efflux pump AcrB. Nat. Struct. Mol. Biol. 2008;15:199-205.
559 [68] Takatsuka Y, Nikaido H. Covalently Linked Trimer of the AcrB Multidrug Efflux
560 Pump Provides Support for the Functional Rotating Mechanism. J. Bacteriol.
561 2009;191:1729-37.
562 [69] Jewel Y, Liu J, Dutta P. Coarse-grained simulations of conformational changes
563 in the multidrug efflux transporter AcrB. Mol. BioSyst. 2017;13:2006-14.
564 [70] Yamane T, Murakami S, Ikeguchi M. Functional Rotation Induced by Alternating
565 Protonation States in the Multidrug Transporter AcrB: All-Atom Molecular Dynamics
566 Simulations. Biochemistry 2013;52:7648-58.
567 [71] Takatsuka Y, Chen C, Nikaido H. Mechanism of recognition of compounds of
568 diverse structures by the multidrug efflux pump AcrB of Escherichia coli. Proc. Natl.
569 Acad. Sci. U. S. A. 2010;107:6559-65.
570 [72] Trott O, Olson AJ. Autodock Vina: Improving the Speed and Accuracy of
571 Docking with a New Scoring Function, Efficient Optimization, and Multithreading. J.
572 Comput. Chem. 2010;31:455-61.

ACCEPTED MANUSCRIPT

573 [73] Husain F, Nikaido H. Substrate path in the AcrB multidrug efflux pump of
574 Escherichia coli. Mol. Microbiol. 2010;78:320-30.
575 [74] Imai T, Miyashita N, Sugita Y, Kovalenko A, Hirata F, Kidera A. Functionality
576 Mapping on Internal Surfaces of Multidrug Transporter AcrB Based on Molecular
577 Theory of Solvation: Implications for Drug Efflux Pathway. J. Phys. Chem. B
578 2011;115:8288-95.
579 [75] Marsh L. Strong Ligand-Protein Interactions Derived from Diffuse Ligand
580 Interactions with Loose Binding Sites. BioMed Res. Int. 2015;2015:6.
581 [76] Kobayashi N, Tamura N, van Veen HW, Yamaguchi A, Murakami S. β-Lactam
582 Selectivity of Multidrug Transporters AcrB and AcrD Resides in the Proximal Binding
583 Pocket. J. Biol. Chem. 2014;289:10680-90.
584 [77] Schlitter J, Engels M, Krüger P, Jacoby E, Wollmer A. Targeted molecular
585 dynamics simulation of conformational change-application to the T↔ R transition in
586 insulin. Mol. Simul. 1993;10:291-308.
587 [78] Grubmüller H, Heymann B, Tavan P. Ligand binding: molecular mechanics
588 calculation of the streptavidin-biotin rupture force. Science 1996;271:997-9.
589 [79] Izrailev S, Stepaniants S, Balsera M, Oono Y, Schulten K. Molecular dynamics
590 study of unbinding of the avidin-biotin complex. Biophys. J. 1997;72:1568-81.
591 [80] Yoshida K-i, Nakayama K, Ohtsuka M, Kuru N, Yokomizo Y, Sakamoto A, et al.
592 MexAB-OprM specific efflux pump inhibitors in Pseudomonas aeruginosa. Part 7:
593 Highly soluble and in vivo active quaternary ammonium analogue D13-9001, a
594 potential preclinical candidate. Bioorg. Med. Chem. 2007;15:7087-97.
595 [81] Nakashima R, Sakurai K, Yamasaki S, Hayashi K, Nagata C, Hoshino K, et al.
596 Structural basis for the inhibition of bacterial multidrug exporters. Nature
597 2013;500:102-6.

ACCEPTED MANUSCRIPT

598 [82] Hénin J, Chipot C. Overcoming free energy barriers using unconstrained
599 molecular dynamics simulations. J. Chem. Phys. 2004;121:2904-14.
600 [83] Bohnert JA, Schuster S, Szymaniak-Vits M, Kern WV. Determination of Real-
601 Time Efflux Phenotypes in Escherichia coli AcrB Binding Pocket Phenylalanine
602 Mutants Using a 1,2'-Dinaphthylamine Efflux Assay. PLoS ONE 2011;6.
603 [84] Bohnert JA, Schuster S, Seeger MA, Fahnrich E, Pos KM, Kern WV. Site-
604 Directed Mutagenesis Reveals Putative Substrate Binding Residues in the
605 Escherichia coli RND Efflux Pump AcrB. J. Bacteriol. 2008;190:8225-9.
606 [85] Schuster S, Kohler S, Buck A, Dambacher C, König A, Bohnert JA, et al.
607 Random Mutagenesis of the Multidrug Transporter AcrB from Escherichia coli for
608 Identification of Putative Target Residues of Efflux Pump Inhibitors. Antimicrob.
609 Agents Chemother. 2014;58:6870-8.
610 [86] Middlemiss JK, Poole K. Differential impact of MexB mutations on substrate
611 selectivity of the MexAB-OprM multidrug efflux pump of Pseudomonas aeruginosa. J.
612 Bacteriol. 2004;186:1258-69.
613 [87] Ohene-Agyei T, Lea JD, Venter H. Mutations in MexB that affect the efflux of
614 antibiotics with cytoplasmic targets. FEMS Microbiol. Lett. 2012;333:20-7.
615 [88] Su C-C, Li M, Gu R, Takatsuka Y, McDermott G, Nikaido H, et al. Conformation
616 of the AcrB Multidrug Efflux Pump in Mutants of the Putative Proton Relay Pathway.
617 J. Bacteriol. 2006;188:7290-6.
618 [89] Müller RT, Travers T, Cha H-j, Phillips JL, Gnanakaran S, Pos KM. Switch loop
619 flexibility affects substrate transport of the AcrB efflux pump. J. Mol. Biol.
620 2017;429:3863-74.
621 [90] Nagano K, Nikaido H. Kinetic behavior of the major multidrug efflux pump AcrB
622 of Escherichia coli. Proc. Natl. Acad. Sci. U. S. A. 2009;106:5854-8.

ACCEPTED MANUSCRIPT

623 [91] Lim SP, Nikaido H. Kinetic Parameters of Efflux of Penicillins by the Multidrug
624 Efflux Transporter AcrAB-TolC of Escherichia coli. Antimicrob. Agents Chemother.
625 2010;54:1800-6.
626 [92] Husain F, Bikhchandani M, Nikaido H. Vestibules Are Part of the Substrate Path
627 in the Multidrug Efflux Transporter AcrB of Escherichia coli. J. Bacteriol.
628 2011;193:5847-9.

ACCEPTED MANUSCRIPT

ACCEPTED MANUSCRIPT

629 ***Figure legends***

630 Fig. 1. Structural features of AcrB. A-B) Side (A) and top (B) view of the structure of
631 the AcrB asymmetric homotrimer. Monomers are shown as ribbons colored solid
632 cyan (L), solid yellow (T) and transparent red (O). The structures of antibiotics and
633 inhibitors co-crystallized at three different binding positions (AP on L monomer [34,
634 37], DP on T monomer [36, 37, 81, 34, 31, 18] and TM1-2 pocket [35]) are also
635 shown with sticks of different colors. C) Subdomains and key elements putatively
636 related to function are shown as colored ribbons in the T monomer (L and O
637 monomers are shown as transparent surfaces). Transparent spheres indicate the
638 approximate positions of TM1-2 pocket (blue), AP (green) and DP (red) as deduced
639 from experimental structures. Residues D407, D408 and K940 lining the proton relay
640 pathway within the TM region are shown as sticks colored according to their type (red
641 and cyan for D and K residues respectively).

ACCEPTED MANUSCRIPT

ACCEPTED MANUSCRIPT

642 Fig. 2 Proposed functional rotation mechanism and substrate extrusion path in RND
643 transporters (adapted from [39]). (A) Top view of the different conformations
644 assumed by AP, DP and Gate during cycles of the functional rotation mechanism.
645 The substrate extrusion path is indicated by short black arrows and the substrate is
646 represented by orange van der Waals spheres. (B) The putative substrate transport
647 pathway from AP to the Gate going through DP, as seen from the periplasmic front,
648 is shown as a thick tube. The parts colored in steel blue and magenta indicate,
649 respectively, the stages of the transport cycle associated with L→T and T→O
650 conformational changes. The substrate is represented by sticks colored green, red or
651 ice blue when interacting with the AP, DP and Gate (also colored green, red or ice
652 blue), respectively. The F617-loop is also shown for reference in yellow.

ACCEPTED MANUSCRIPT

ACCEPTED MANUSCRIPT

Fig. 3. Water channels identified in all-atom simulations within the TM domain of different monomeric conformational states in AcrB (adapted from [36]). The water channels (solid black lines) are represented by average density maps and depicted as an iso-density surface (gray). The narrow dashed black line seen in monomer T represents the blocked water channel connecting the proton-binding site to the cytoplasm and traversed by the positively charged R971. TM helices are represented as cartoons colored differently according to their topological helical repeats, and helices TM7, TM9 and TM12 are omitted for clarity. The locations of Cα atoms of D407, D408, K940, R971, E346 and D924 are marked with green spheres.

ACCEPTED MANUSCRIPT

ACCEPTED MANUSCRIPT

Fig. 4. Multifunctional character of the DP of AcrB (adapted from [46]). A) Residues interacting favorably with substrates of the AcrB transporter in [46]. Residues are shown with sticks whose width is proportional to the frequency of binding contacts with the ligands. The DP, AP, Cleft and AP/DP interface are shown in red, green, orange and yellow transparent surfaces, respectively. The tip of the Phe617-loop is also shown in yellow cartoon. Bold labels refer to residues contributing to stabilizing binding of at least three substrates (inhibitors or not) of AcrB. The dark red line highlights the contour of the DP according to this analysis. B) Frequency of contribution to binding free energy of substrates by hydrophobic (black bars), polar (green) and charged (red) residues. The sum over all frequencies is reported above each histogram.

ACCEPTED MANUSCRIPT

ACCEPTED MANUSCRIPT

673 Fig. 5. MFSs identified within the putative binding pockets (AP and DP) of AcrB and
674 AcrD (adapted from [39]). The binding modes of the different probes are shown as
675 lines for hydrogen-bond donor (cyan), hydrogen-bond acceptor (violet) and aliphatic
676 (yellow), and as CPK for aromatic (ochre) ligands. The AP and DP are marked in
677 green and red cartoon representations, respectively, and the Phe617-loop in yellow.
678 The sites not labelled as MFS are all consensus sites (i.e. clusters of the same
679 probe type). The location-based grouping of MFSs is arbitrary due to indistinct
680 boundaries between the pockets.

ACCEPTED MANUSCRIPT

ACCEPTED MANUSCRIPT

Fig. 6. Ligand-dependent drug uptake pathways in AcrB (adapted from [56]). (A) The three principal drug uptake pathways identified in AcrB. The Vestibule pathways are shown in blue and the Cleft pathway is shown in orange. The residues lining the Vestibule and Cleft are shown as beads colored in blue and orange, respectively. The Phe617-loop is also shown for reference in yellow. (B) The difference in the activation-free energy of drug uptake in monomer T, $\Delta\Delta E_{\varphi} = \Delta E_{\varphi}^{\text{vestibule}} - \Delta E_{\varphi}^{\text{cleft}}$, on two-dimensional (2D) hydrophobicity (c_P) and lipophilicity (c_M) space of the drug. The activation-free energy $\Delta E_{\varphi}^{\text{vestibule}}$ and $\Delta E_{\varphi}^{\text{cleft}}$ represents the barrier from the membrane to the AP through the Vestibule and Cleft pathways, respectively.

ACCEPTED MANUSCRIPT

ACCEPTED MANUSCRIPT

690 Fig 7. Effect of the F610A mutation on binding of doxorubicin [48]. A) The substrate
691 is shown in sticks colored accordingly to the atom type. Side chains of
692 phenylalanines lining the hydrophobic trap are shown with light purple sticks. Two
693 yellow lines schematically enclose the transport channel, with the arrow indicating the
694 direction of efflux. The blue line delimits the hydrophobic trap. A) Doxorubicin bound
695 to the DP of AcrB (from X-ray structure 4DX7 [37]). Phenylalanines within 3.5 Å of
696 the ligand are shown with thicker sticks. B) Doxorubicin sliding within the hydrophobic
697 trap in the F610A AcrB variant [48]. The position of the drug in the WT protein is
698 shown with thin gray sticks to highlight the reorientation and embedding of the
699 antibiotic within the hydrophobic trap.

ACCEPTED MANUSCRIPT

ACCEPTED MANUSCRIPT

Tables

Region	Lining residues
DP	S46 **Q89** S128 E130 **S134** **F136 Q176** L177 **F178** S180 E273 **N274 D276 I277 G290 Y327** **M573** F610 V612 **F615** **F617** **R620 F628**
AP	S79 T91 **S134** S135 K292 **M573** M575 Q577 **F617** T624 M662 *F664 F666* N667 *L668 P669 V672* L674 *T676* D681 *R717* N719 E826
TM1-2	I27 K334 I337 H338 V341
Cleft	**D566** ***F664 F666 L668*** *P669 V672* ***E673 T676 R717*** **L828**
Vestibule	**S836 E842 L868 Q872**
Gate	**Q124** Q125 **Y758**

Table 1. Residues identifying key regions of AcrB involved in substrate uptake and extrusion (as deduced from experimental structures of the asymmetric transporter in complex with substrates and inhibitors [73, 92, 31, 34, 35, 18, 37]). Residues shared by the Cleft and the AP are italicized, while those shared between the AP and DP are underlined. Residues identified as part of the extrusion path of AcrB substrates are bolded.

ACCEPTED MANUSCRIPT

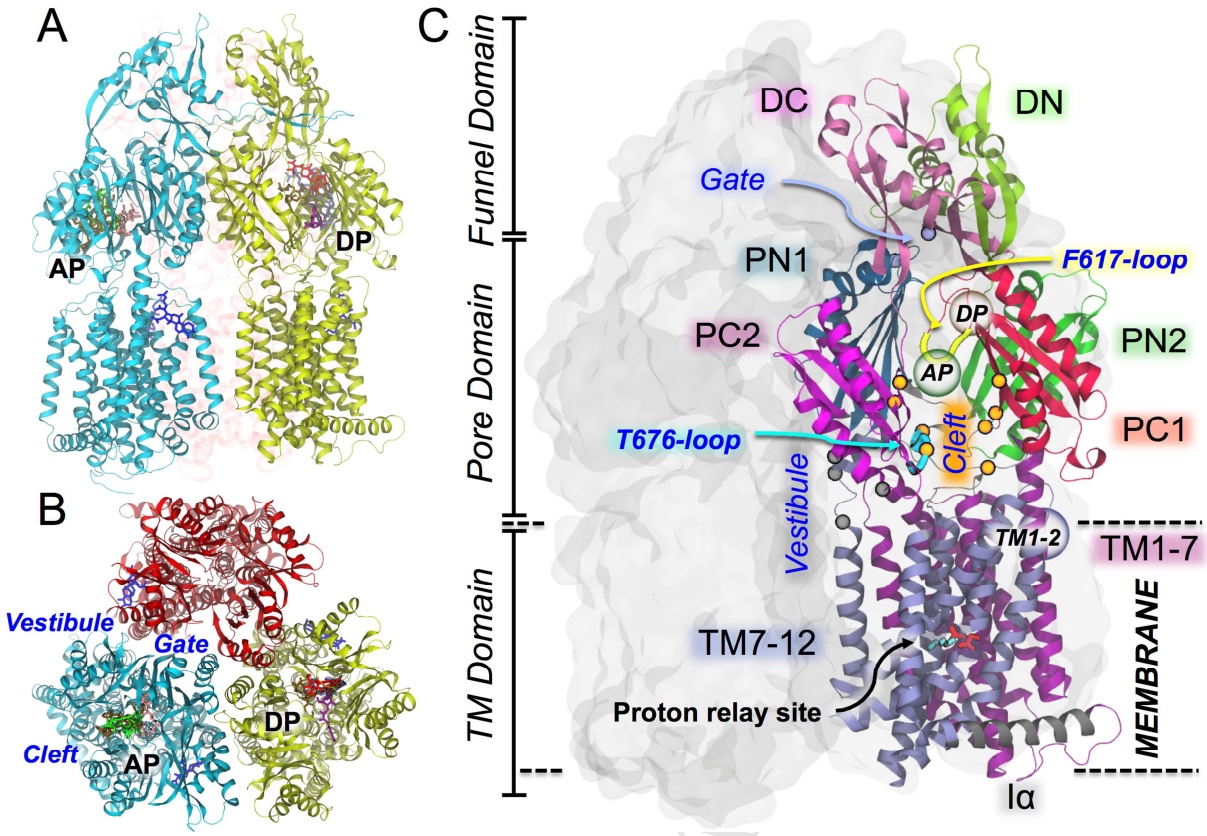

ACCEPTED MANUSCRIPT

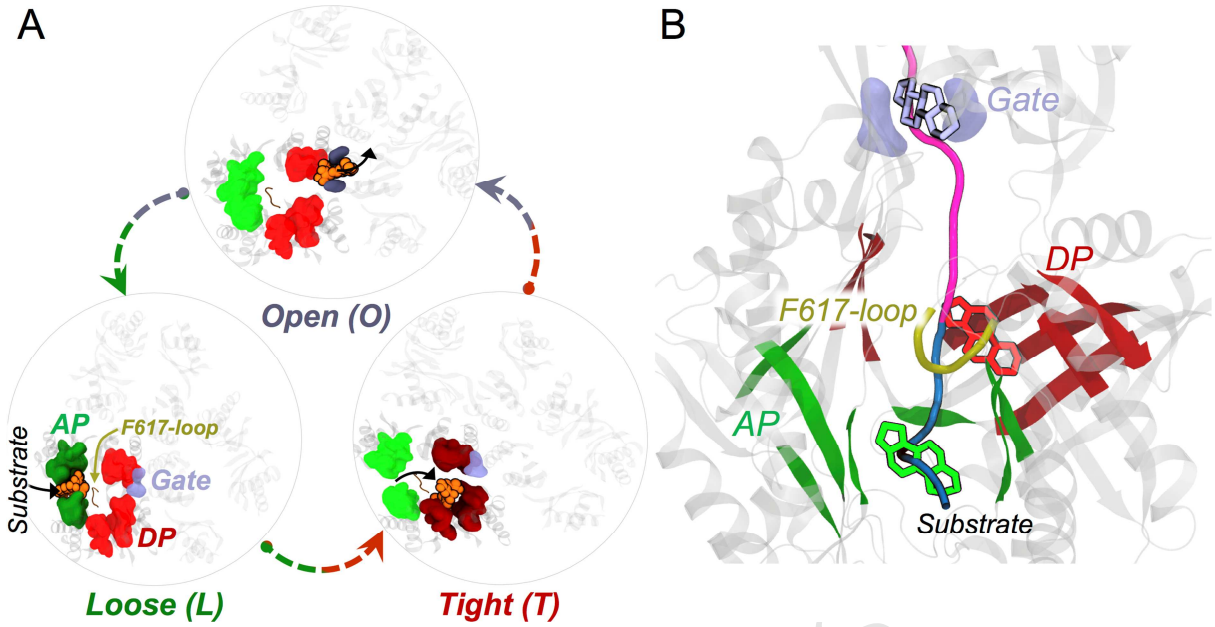

ACCEPTED MANUSCRIPT

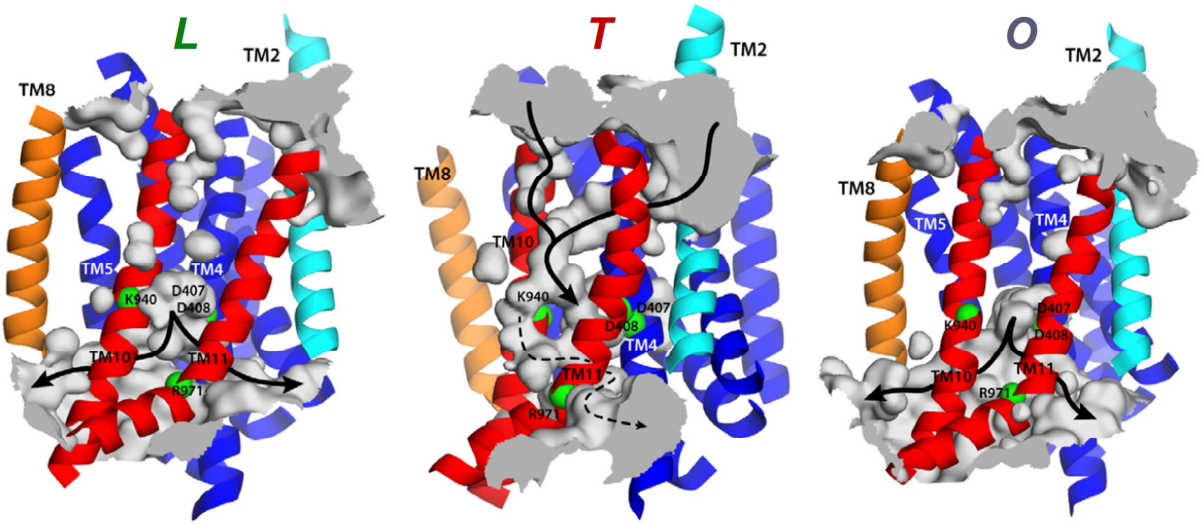

ACCEPTED MANUSCRIPT

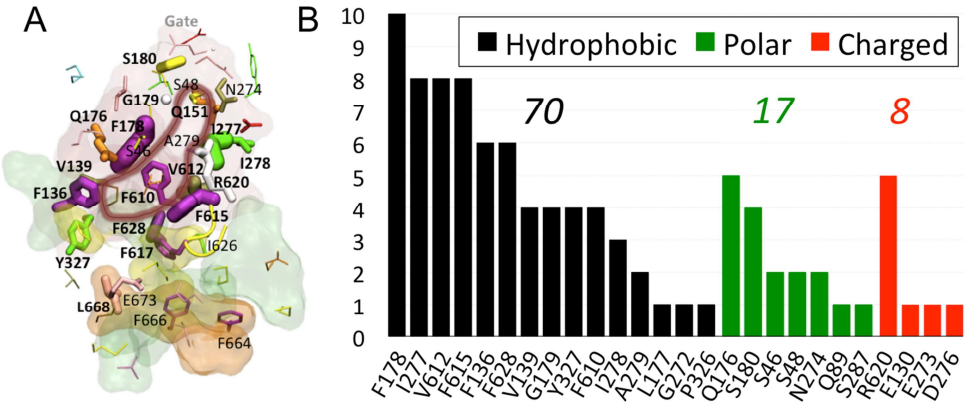

ACCEPTED MANUSCRIPT

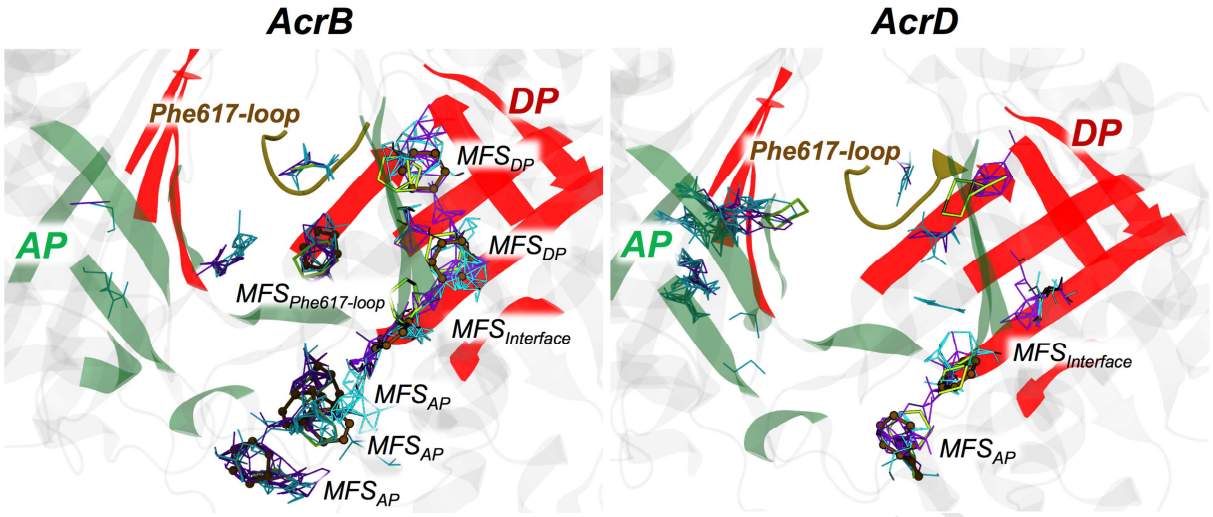

ACCEPTED MANUSCRIPT

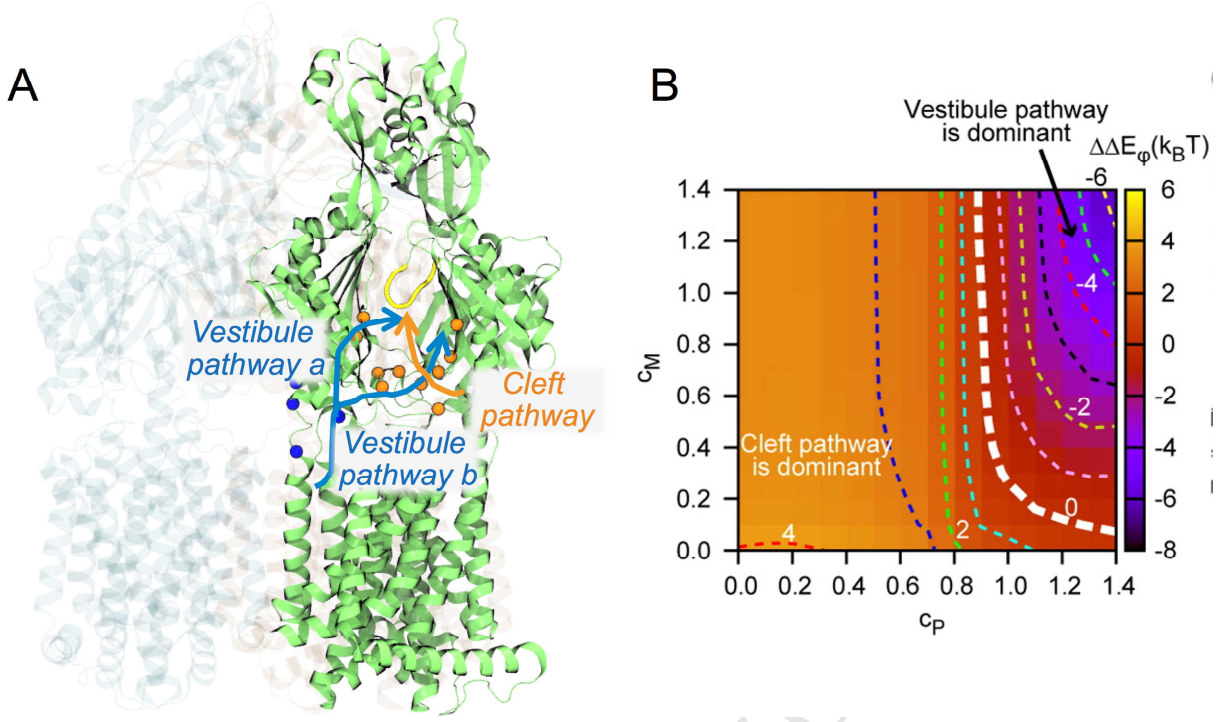

ACCEPTED MANUSCRIPT

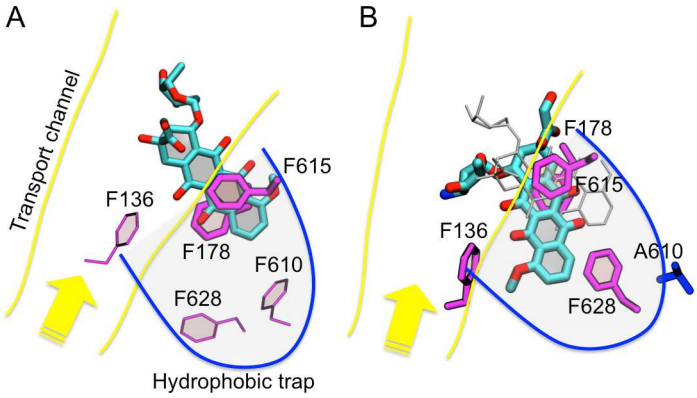

ACCEPTED MANUSCRIPT